Asymmetric vortex merger: Experiments and simulations

M. Amoretti
Istituto Nazionale di Fisica della Materia, Dipartimento di Fisica, Università degli Studi di Milano, Via Celoria 16, 20133 Milano, Italy

D. Durkin and J. Fajans
Department of Physics, University of California at Berkeley, Berkeley, California 94720-7300

R. Pozzoli and M. Romé
Istituto Nazionale di Fisica della Materia, Dipartimento di Fisica, Università degli Studi di Milano, Via Celoria 16, 20133 Milano, Italy

(Received 23 April 2001; accepted 14 June 2001)

The two-dimensional (2-D) merging of an intense, pointlike vortex with a diffuse, extended vortex is investigated with experiments using strongly magnetized electron columns in a Malmberg–Penning trap, and with numerical simulations using a 2-D particle-in-cell code. The study is restricted to highly nonlinear conditions, where the perturbative approach does not apply. A very good agreement between experiment and simulation is obtained. The pointlike vortex wraps the extended vortex about itself, moving toward the center of the system during the process. The interaction generates filaments of zero vorticity within the extended vortex that subsequently evolve into vorticity holes. During the evolution, energy is fed to the extended vortex from the background curl-free flow via the stirring action of the pointlike vortex, whose energy remains approximately constant. © *2001 American Institute of Physics.* [DOI: 10.1063/1.1390331]

The merger of two vortices is a fundamental interaction in two-dimensional (2-D) flows. It plays a prominent role in the evolution of 2-D turbulence,[1] and has been observed in the ocean between eddies[2] and on Jupiter between anticyclones.[3] The two vortices will likely have different sizes and vorticities, and therefore the merger will be asymmetric,[4–8] as opposed to symmetric.[9,10]

The highly asymmetric case of an intense, pointlike vortex merging with a diffuse, extended vortex is considered. The vortices are constrained to be initially circular with radii $a_{p,e}$ and uniform with vorticities $\zeta_{p,e}$, where p,e denote pointlike and extended. The case $a_p \ll a_e$ and $\zeta_p \gg \zeta_e$ is addressed. The merger can be parametrized by Γ_p/Γ_e, d/a_e, and a_p/a_e, where $\Gamma=\pi a^2\zeta$ is the circulation and d is the distance between their centers. The merger is governed by the 2-D Euler equations,

$$\partial\zeta/\partial t+\mathbf{u}\cdot\boldsymbol{\nabla}\zeta=0, \quad \mathbf{u}=\mathbf{e}_z\times\boldsymbol{\nabla}\psi, \quad \nabla^2\psi=\zeta, \tag{1}$$

where $\zeta\equiv\mathbf{e}_z\cdot\boldsymbol{\nabla}\times\mathbf{u}$ and ψ is the stream function. The boundary condition is free-slip with $\psi=0$ on a circular wall ($r=R_w$).

Mathematical analysis of 2-D vortex merger has proven intractable. For the case under consideration, the linear analysis of Ref. 7 is not valid because the extended vortex is soon highly distorted from its initial circular shape. One has to therefore rely upon numerical simulation or experiment.

Results from contour dynamics simulations in an unbounded domain are reported in Refs. 4 and 6. In particular, Fig. 13 in Ref. 4 depicts a case similar to the present one, and there it is noted that the pointlike vortex is ''entrained'' within the extended vortex. Contour dynamics, however, fails once vorticity filaments evolve and therefore the later dynamics were not pursued. Reference 5 also presents a similar case, this time simulated with a pseudospectral code in a periodic domain; therein is reported the emergence of vorticity holes, in qualitative agreement with the present observations.

Experiments on 2-D vortex merger, and on 2-D fluid dynamics in general, are hindered by the difficulty in creating the desired initial conditions. Reference 11 reports limited observations of asymmetric vortex merger in a rotating water tank, but those experiments were also hampered by viscous and boundary effects. Experiments on merger of almost equal vortices using strongly magnetized electron columns were first reported in Ref. 12. Reference 13 discusses experiments on the merger of nonuniform vortices with the same peak vorticities and different sizes.

The present experiments also use strongly magnetized electron columns confined within a Malmberg–Penning trap, but equipped with a photocathode electron source (see Fig. 1). This setup has already been used to study the dynamics of a pointlike vortex inside an extended vortex.[14] Under suitable conditions, the dynamics of the electron column perpendicular to the imposed magnetic field are equivalent to those of an ideal 2-D fluid.[15] The vorticity, ζ, is proportional to the electron density, n, and is given by $\zeta=(4\pi ec/B)n$, where B is the magnetic field strength; hence, a strongly magnetized electron column behaves like an ideal 2-D vortex.

Figure 2 in the first column presents the experimental observations for the case of $\Gamma_p/\Gamma_e=0.15$ and $d/a_e=1.41$; specifically, $a_p=0.07$ cm, $\zeta_p=4.3\times10^4\ \mathrm{s}^{-1}$ ($n_p=6.8\times10^6\ \mathrm{cm}^{-3}$), $a_e=0.60$ cm, $\zeta_e=3.9\times10^3\ \mathrm{s}^{-1}$ ($n_e=6.2\times10^5\ \mathrm{cm}^{-3}$), and $d=0.85$ cm (the wall is 2.00 cm from the center of the extended vortex). The pointlike vortex distorts

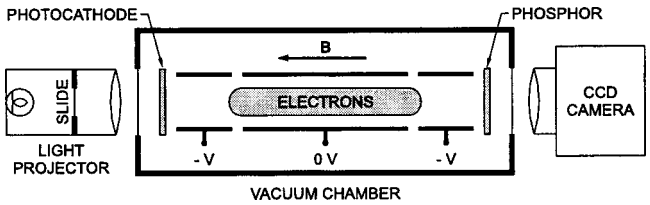

FIG. 1. The Malmberg–Penning trap (Ref. 19) consists of three coaxial, conducting cylinders contained within a high vacuum chamber. The electron columns are confined radially with a static magnetic field ($B=3$ T) and axially with electric fields ($-V$ is the confining potential). The desired initial 2-D electron distribution is created by projecting the appropriate light image onto a cesium antimonide photocathode (Ref. 20) and grounding the left cylinder; electrons are emitted only where there is light, and they stream along the magnetic field lines into the central confinement region, preserving their distribution. The electrons are confined by applying a negative electric potential to the left cylinder. The distribution is allowed to evolve for a given time, after which the right cylinder is grounded and the electrons are destructively imaged by streaming them onto a phosphor screen. A charge coupled device camera detects the resulting image. The image's intensity is proportional to the electron density, and therefore to the vorticity.

the extended vortex, wrapping the extended vortex about itself. In the process, filaments of zero vorticity are entrained within the extended vortex. These filamentary voids behave as filaments of negative vorticity and subsequently evolve via the Kelvin–Helmholtz instability into vorticity holes. At late times, the pointlike vortex is centered within a vorticity hole and found close to the extended vortex's center; about it orbit several vorticity holes.

The numerical simulations are performed with the 2-D (in real space) particle-in-cell (PIC) code known as XOOPIC.[16] This code enables us to pursue the dynamics to longer times compared to contour dynamics. Moreover, it accounts for the circular boundary, which affects the orbits of the two vortices. The parameters of the simulation are the same as in the experimental situation. In particular, note that no free parameter is introduced. The number N of macroparticles used in the simulations is $\lesssim 10^5$ with a 256×256 square grid. The stability of the results with respect to variations of N and grid size has been verified. The results obtained by PIC simulations for the reference case are shown always in Fig. 2. The good agreement between experimental data and simulation shows that the behavior of the system is indeed 2-D Eulerian, even in this highly nonlinear regime; this confirms the potentiality of Malmberg–Penning traps for fluid dynamics experiments.

Various experiments have been carried on with different values of a_p/a_e, d/a_e, and Γ_p/Γ_e, in the range $0.02<\Gamma_p/\Gamma_e<0.4$. The corresponding numerical simulations show in all cases good agreement: differences are found only in the late phase of the motion, where the spiral channel goes unstable and vorticity holes form. In Fig. 3 it is shown as an example the comparison between experiment and simulation for the merger time for different values of the circulation ratio, and fixed d. In both cases, the pointlike vortex is considered to be merged when its radial position becomes equal to a_e. The slight difference at small values of the circulation ratio, where the small vortex tends to be sheared out by the extended one, may be due to a nonuniformity of the profile of the pointlike vortex in the experiment.

If Γ_p/Γ_e is sufficiently small, during the first phase of motion the pointlike vortex is simply conveyed with a good approximation by the velocity field produced by the extended vortex, which necessarily exhibits shear. Because the pointlike vortex is assumed to have a small but finite radius, it is necessary to take into account a possible deformation of its shape. This deformation is governed by the balance between rotation coming from its own vorticity and straining caused by the mentioned velocity field of the extended vortex.[17] For a fixed value of a_e, this process is regulated, e.g., by the parameter $K\equiv(\Gamma_p/\Gamma_e)(d/a_p)^2$. Depending on the value of K, different outer fractions of the pointlike vortex are affected by filamentation, while merger eventually occurs for the remaining core part.

If K is large enough ($K\gtrsim 4$), the filamentation of the pointlike vortex is avoided, and merger occurs via a rapid wrapping process. The following discussion refers to merger under the above-mentioned conditions, where the pointlike vortex has a small circulation with respect to the extended vortex, and maintains its shape during the motion.

For very small circulation ratios ($\Gamma_p/\Gamma_e\lesssim 0.01$) small amplitude Kelvin (surface) waves are induced, and "falling" of the pointlike vortex toward the extended vortex occurs due to a resonance overlapping mechanism.[7] In the cases under consideration here the merger process is faster, the merging times shown in Fig. 3 are shorter, and the cited theory does not apply.

The present investigation indicates that during merger the stream function ψ approaches a smooth function with a single maximum, which rotates around the center of the system. The early phase of merger can be conveniently described in a reference frame rotating with the angular velocity of the pointlike vortex, $\Omega_p\approx\Gamma_e/(2\pi d^2)$. In this frame the pointlike vortex rotates around itself, and shows only small deformations of its shape; the motion of the extended vortex can then be inferred from the behavior of the field lines of the stream function in the rotating frame, $\overline{\psi}=\psi-\Omega_p(r^2-R_w^2)/2$. For the reference case the contour lines of the corotating potential are shown in Fig. 2.

If K is not too large, the $\overline{\psi}$ field initially exhibits an X point located between the two vortices, and the relevant separatrix crosses the extended vortex. The part of this vortex lying outside the separatrix gives rise to the wrapping process [see plot (a) of the corotating potential in Fig. 2]. The presence of the mentioned X point also determines the shape of the extended vortex during the initial phase of wrapping [see plot (b) in Fig. 2], and allows phase space mixing of fluid elements in its surrounding.[18] The separatrix encircles the pointlike vortex with no crossing, and this vortex is unaffected by strain.

As wrapping develops, vorticity from the extended vortex accumulates around the pointlike vortex, leading to the coalescence of the X point with the O point associated with the extended vortex. For the given initial conditions, this change in the phase space characterizes the occurrence of merging. An annular region of zero vorticity around the pointlike vortex forms. This region increases with increasing K. This feature persists during the evolution, and shows that

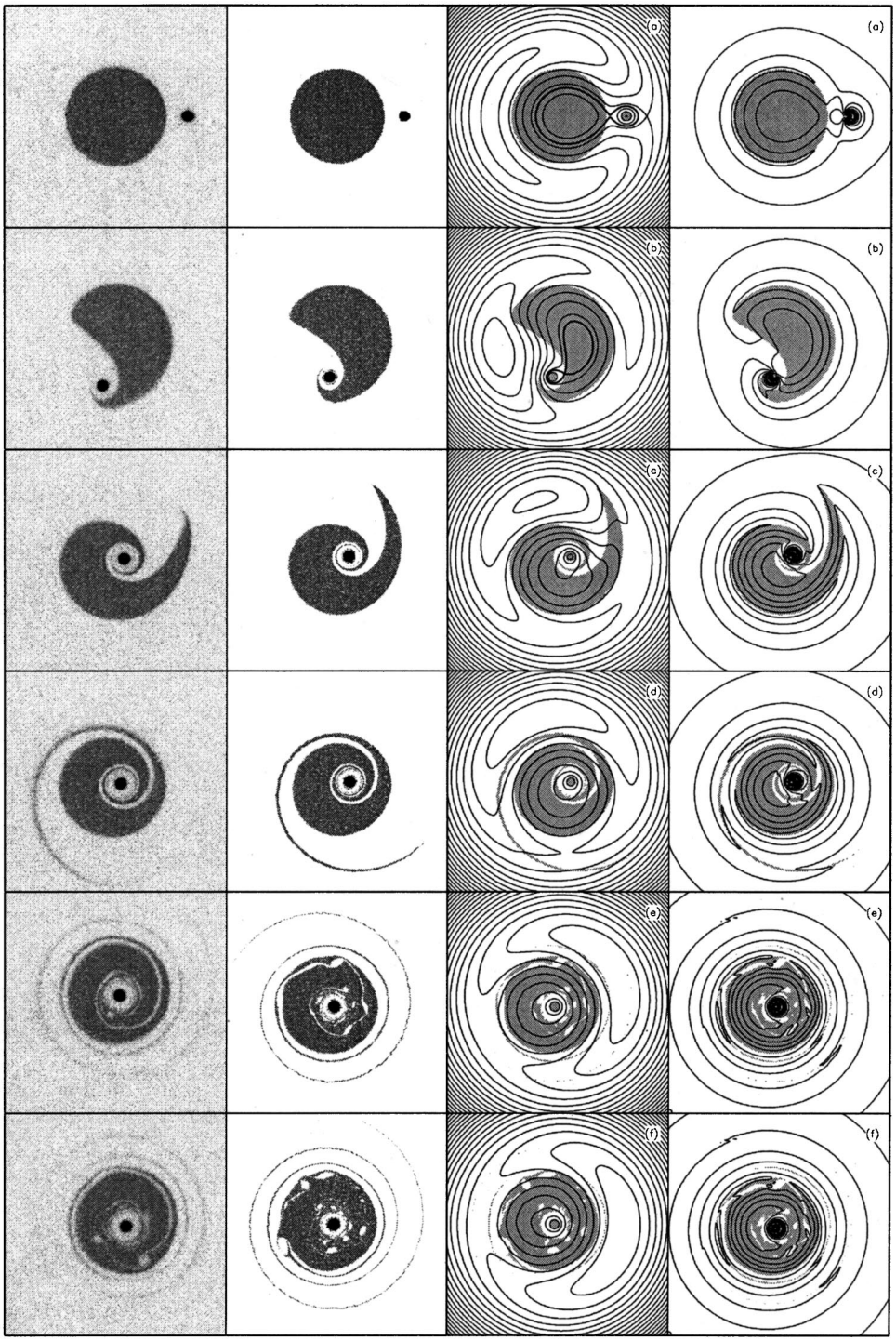

FIG. 2. Time evolution of the interaction of a point vortex with an extended vortex. From top to bottom, the data refer to $t=0.0$, 0.5, 1.0, 2.0, 4.0, and 5.0, respectively, with the time measured in units of the period of rotation of the extended vortex, $4\pi/\zeta_e$. First column: density (experimental results). Second column: density (PIC simulation). Third column: contour plot of the corotating potential $\overline{\psi}$ (PIC simulation). The thick line represents the separatrix crossing the extended vortex. Fourth column: contour plot of the fluid energy density ϵ (PIC simulation). The lengths are normalized over R_w.

the dynamics of the system is qualitatively different from that of a point vortex within a vortex studied in Ref. 14.

Wrapping leads to the formation of a spiral, zero vorticity channel, and to the filamentation of the extended vortex, due to the straining and the rotation induced by the vorticity distribution around the pointlike vortex. During wrapping the width of the channel decreases, and a Kelvin–Helmholtz instability may arise. This leads to the formation of holes, i.e., localized regions of zero vorticity, inside the extended vortex, with effective reconnection of the vorticity field. The mentioned features are shown in Fig. 2 [plots from (c) to (f)].

At smaller K values, the X point is initially shifted toward the center of the pointlike vortex, and strain begins to play a role. At larger K, the initial condition does not show a separatrix between the two vortices: all field lines crossing the extended vortex encircle the pointlike vortex, and merger occurs rapidly with the formation of a large region of zero vorticity surrounding the pointlike vortex.

The above-mentioned investigation points out that during the merger, the pointlike vortex exerts a stirring action on the fluid as it migrates towards the center of the system. This stirring process is illustrated by considering the behav-

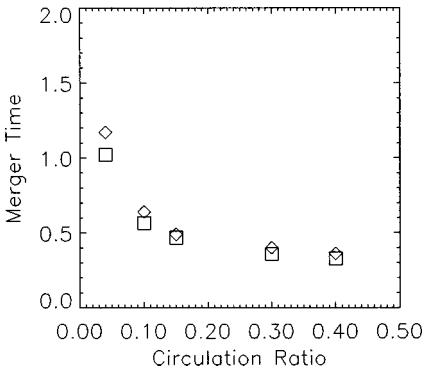

FIG. 3. Merger time vs circulation ratio, Γ_p/Γ_e. The time is measured in units of the period of rotation of the extended vortex, $4\pi/\zeta_e$. Diamonds and squares denote experimental and simulation results, respectively. In all cases, $d=0.85$ cm, $a_e=0.60$ cm, and $n_e=6.2\times10^5$ cm^{-3}. The circulation ratio is varied by changing the radius of the pointlike vortex (keeping $a_p \leqslant 0.12$ cm) and/or its density.

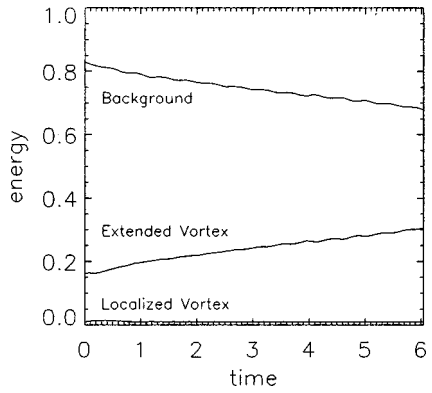

FIG. 4. Time evolution of the total fluid energy of the two vortices and the background (PIC simulation). The data are the same as in Fig. 2.

ior of the kinetic energy density of the fluid $\epsilon(x,y,t)=\frac{1}{2}|\nabla\psi|^2$, whose contour plots are shown in the last column of Fig. 2 (in the plasma language this corresponds to the energy density of the electric field). The total energy of the system, E, is a constant of motion, and reads

$$E=\frac{1}{2}\int_S|\nabla\psi|^2dS=\sum_i E_i, \tag{2}$$

where the integration is made over the whole space within the circular boundary, and E_i with $i=e,v,b$ represents the energies associated with the extended vortex, the pointlike vortex, and the background, respectively. The energy density is initially concentrated near the boundaries of the two vortices, while in the region around the hyperbolic point of ψ, it has a local minimum. The wrapping process leads to stirring of the background curl-free flow. The behavior of the fluid energy in the region of the two vortices and in the background is shown in Fig. 4. During the whole process the energy associated to the pointlike vortex does not change significantly, while the energy associated to the extended vortex increases almost linearly in time, at the expense of the background. Note that in conditions where the small vortex is sheared apart, i.e., it does not behave as pointlike (K is small), its energy is exchanged with that of the background while the energy of the extended vortex maintains itself almost constant.

In conclusion, it has been shown by means of experimental evidence and simulation modeling that merger of a pointlike vortex with an extended vortex in the specified nonlinear regime occurs via a wrapping process leading to a new vorticity distribution with the pointlike vortex, that has maintained its shape during the whole process, at its center. The surrounding vortex has the shape of a rotating and straining spiral, where at late time vorticity holes form and mixing with the surrounding zero vorticity fluid (background) occurs. During the merger, energy is transferred from the background fluid to the extended vortex via the stirring action of the pointlike vortex.

ACKNOWLEDGMENT

This work was partially supported by the Office of Naval Research.

[1] J. C. McWilliams, J. Fluid Mech. **219**, 361 (1990).
[2] G. R. Cresswell, Science **215**, 161 (1981).
[3] A. Sanchez-Lavega, J. F. Rojas, R. Hueso, J. Lecacheux, F. Colas, J. R. Acarreta, I. Miyazaki, and D. Parker, Icarus **142**, 116 (1999).
[4] E. A. Overman and N. J. Zabusky, Phys. Fluids **25**, 1297 (1982).
[5] M. V. Melander, N. J. Zabusky, and J. C. McWilliams, Phys. Fluids **30**, 2610 (1987).
[6] D. G. Dritschel and D. W. Waugh, Phys. Fluids A **4**, 1737 (1992).
[7] I. M. Lansky, T. M. O'Neil, and D. A. Schecter, Phys. Rev. Lett. **79**, 1479 (1997).
[8] I. Yasuda and G. R. Flierl, Dyn. Atmos. Oceans **26**, 159 (1997).
[9] M. V. Melander, N. J. Zabusky, and J. C. McWilliams, J. Fluid Mech. **195**, 303 (1988).
[10] A. H. Nielsen, X. He, J. Juul Rasmussen, and T. Bohr, Phys. Fluids **8**, 2263 (1996).
[11] R. W. Griffiths and E. J. Hopfinger, J. Fluid Mech. **178**, 73 (1987).
[12] C. F. Driscoll and K. S. Fine, Phys. Fluids B **2**, 1359 (1990).
[13] T. B. Mitchell and C. F. Driscoll, Phys. Fluids **8**, 1828 (1996).
[14] D. Durkin and J. Fajans, Phys. Rev. Lett. **85**, 4052 (2000).
[15] R. H. Levy, Phys. Fluids **8**, 1288 (1965).
[16] J. P. Varboncoeur, A. B. Langdon, and N. T. Gladd, Comput. Phys. Commun. **87**, 199 (1995).
[17] J. Weiss, Physica D **48**, 273 (1991).
[18] E. A. Novikov, Phys. Lett. A **152**, 393 (1992).
[19] J. H. Malmberg and J. S. deGrassie, Phys. Rev. Lett. **35**, 577 (1975).
[20] D. Durkin and J. Fajans, Rev. Sci. Instrum. **70**, 4539 (1999).